

1 SUPPLEMENTARY INFORMATION

2 **Towards Building Blocks for Supramolecular**
3 **Architectures Based on Azacryptates**4 Ana Miljkovic¹, Sonia La Cognata^{1,*}, Greta Bergamaschi², Mauro Freccero¹, Antonio Poggi¹ and
5 Valeria Amendola¹6 ¹Department of Chemistry, Università degli Studi di Pavia, via Taramelli 12, 27100, Pavia (Italy);7 ² Consiglio Nazionale Delle Ricerche, Istituto di Chimica Del Riconoscimento Molecolare (ICRM), via M.
8 Bianco 9, 20131, Milano (Italy).9 * Correspondence: sonia.lacognata01@universitadipavia.it10 **Index:**11 **Contents**

12	Index:.....	1
13	1. Synthesis.....	2
14	1.1. Synthesis of L.....	2
15	1.2. Synthesis of [Cu ₂ L](CF ₃ SO ₃) ₄	2
16	2. Studies in Solution.....	3
17	2.1. pH-Spectrophotometric Titration of [Cu ₂ L](CF ₃ SO ₃) ₄	3
18	2.2. UV-Vis Titrations of [Cu ₂ L](CF ₃ SO ₃) ₄	3
19	2.3 Emission Studies	5
20	3. Computational Studies	7
21	4. Characterization of [Cu ₂ L] ⁴⁺ by ESI-MS	9
22	5. NMR Characterization of L.....	12
23	References	15

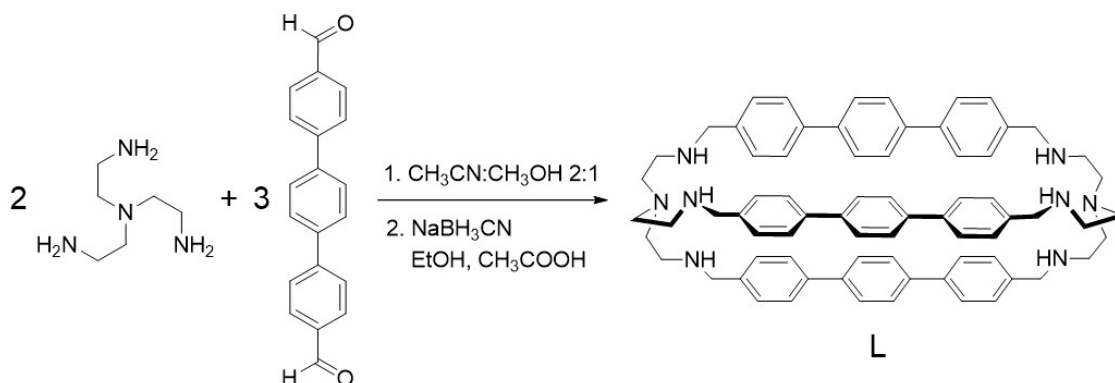
24

25

26 1. Synthesis

27 All reagents and solvents were purchased from Sigma-Aldrich and used without further
 28 purification. [1,1':4,1''-Terphenyl]-4,4''-dicarboxaldehyde was synthesized according to a known
 29 procedure [1]. In the synthesis of L, NaBH₃CN was employed a reducing agent for imine bonds [2].

30 1.1. Synthesis of L



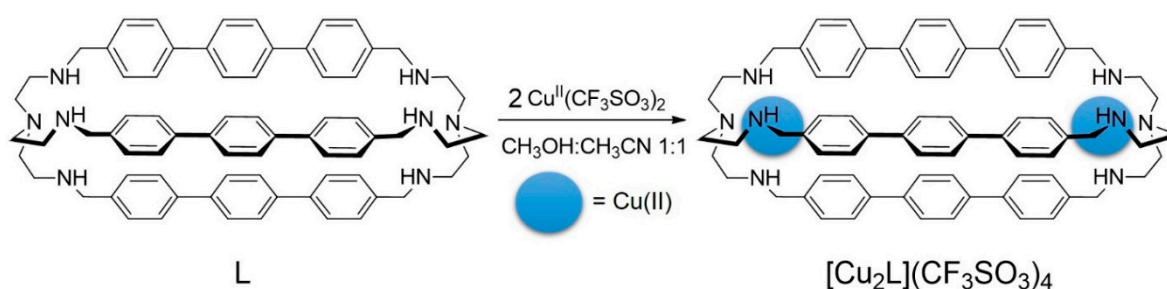
31

32

33 One-hundred milligrams of [1,1':4,1''-Terphenyl]-4,4''-dicarboxaldehyde (100 mg, 0.35 mmol) in
 34 60 mL of 2:1 CHCl₃:MeOH were added to a solution of tren (36 μ l, 0.35 mmol) in 120 mL of the same
 35 medium. The reaction mixture was stirred for 24 hrs at RT, before taking to dryness. The solid residue
 36 was suspended in 100 mL EtOH and dissolved by addition of CH₃COOH. The imine bonds are
 37 reduced by addition of NaBH₃CN (3 eqv. per C=N) to the mixture at RT. The solution is then stirred
 38 at 50 °C overnight. After basification with excess NaOH(aq), EtOH is evaporated and the aqueous
 39 layer is extracted with CHCl₃ (10 \times 25 mL). The reunited organic phases are dried over anhydrous
 40 Na₂SO₄. After evaporation, a white solid is obtained. Yield: 70%. ¹H-NMR (d₆-DMSO + 1M CF₃SO₃H
 41 in D₂O, 400 MHz) δ 7.61 (12H, d, H-a), 7.49 (12H, s, H-e), 7.34 (12H, d, H-b), 4.20 (12H, s, H-3), 3.12
 42 (12H, s, H-2), 2.76 (12H, s, H-1). ¹³C-NMR (d₆-DMSO + 1M CF₃SO₃H in D₂O, 100 MHz), δ 139.04 (6C,
 43 C-q₂), 137.44 (6C, C-q₃), 130.04 (6C, C-q₁), 129.69 (12C, C-b), 126.37-126.14 (24C, C-a, C-c), 48.99 (12C,
 44 C-3), 48.62 (12C, C-1), 42.70 (12C, C-2). ESI-MS (MeOH) *m/z* 528.7 [M+2H]²⁺. Elemental analysis
 45 calculated for C₇₂H₇₈N₈: C, 81.93; H, 7.45; N, 10.62%. Found: C, 81.85; H, 7.63; N, 10.52%.

46

47 1.2. Synthesis of [Cu₂L](CF₃SO₃)₄



48

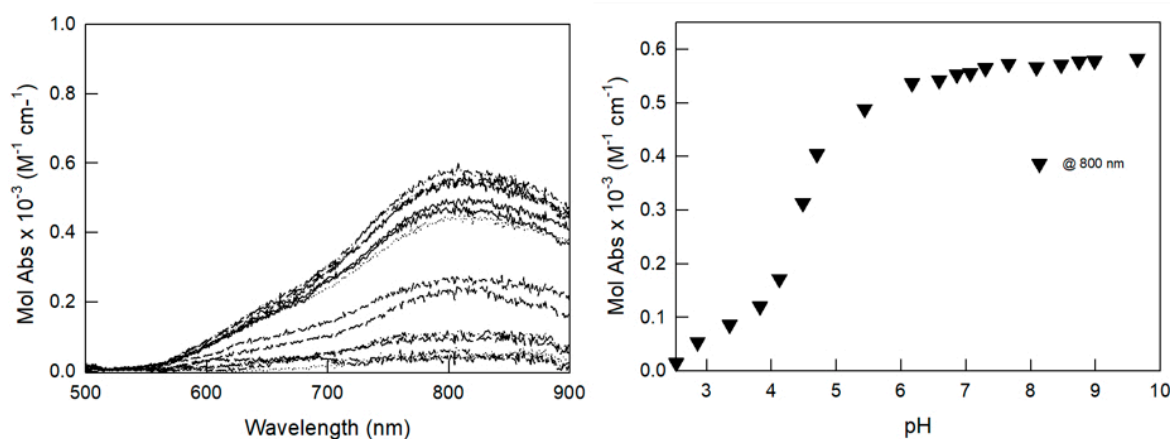
49

To begin, 55.1 mg (0.052 mmol) of L are suspended in 40 mL of MeOH:CH₃CN 1:1 (*v/v*) mixture. Then, 38.3 mg Cu^{II}(CF₃SO₃)₂ (0.107 mmol) in 5 mL MeOH are added, and the obtained solution is refluxed for 3 hrs. After filtering, the solvent is evaporated, and the solid residue is treated with Et₂O. A light green powder is obtained. Yield: 67%. ESI-MS (MeOH) *m/z* 590.22 [Cu^{II}₂(L-2H⁺)]²⁺, *m/z* 665.16 [Cu^{II}₂(L-H+CF₃SO₃)]²⁺ and *m/z* 740.04 [Cu^{II}₂L(CF₃SO₃)₂]²⁺. Elemental analysis calculated for [Cu^{II}₂(C₇₂H₇₈N₈)(CF₃SO₃)₄].1H₂O C, 50.80; H, 4.48; N, 6.24%. Found: C, 50.57; H, 4.59; N, 6.35%.

2. Studies in Solution

2.1. pH-Spectrophotometric Titration of [Cu₂L](CF₃SO₃)₄

pH-spectrophotometric titrations were performed on a 0.2 mM solution of [Cu₂L](CF₃SO₃)₄ in CH₃CN:H₂O 4:1 mixture (NaCF₃SO₃ 0.05 M), 25 °C. In a typical titration, aliquots of carbonate-free standard 0.1 M NaOH were added to the solution of the azacryptate, both the electrochemical potential and the UV-Vis spectrum of the solution were recorded after each addition. Prior to the titration, the standard electrochemical potential (E°) was determined by the Gran method [3].



63

Figure S1. pH-spectrophotometric titration (left) and profile at 800 nm (right) of [Cu₂L](CF₃SO₃)₄.

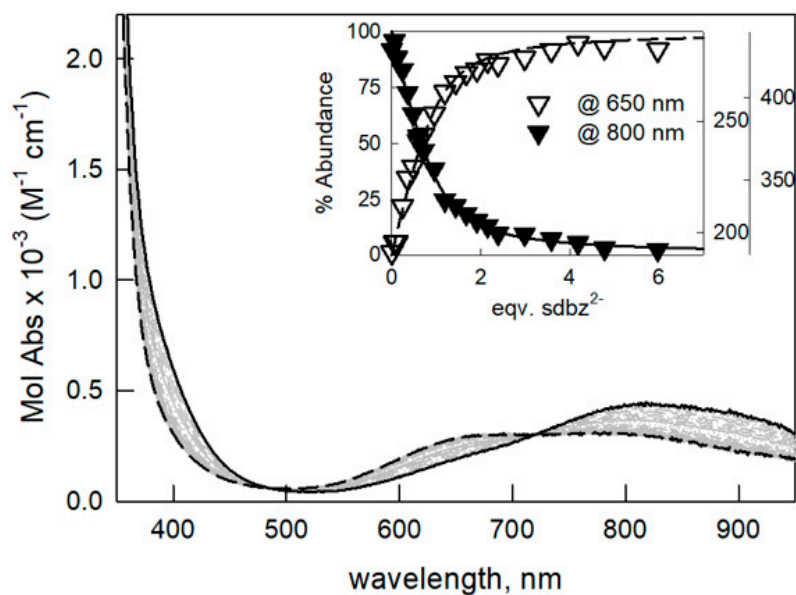
64

2.2. UV-Vis Titrations of [Cu₂L](CF₃SO₃)₄

UV-Vis titrations of [Cu₂L](CF₃SO₃)₄ with biphenyl-4,4'-dicarboxylate (dfc²⁻), 4,4'-sulfonyldibenzoate (sdbz²⁻), terephthalate (tph²⁻) and benzoate (bz⁻) TBA salts were performed in 1:4 (*v:v*) water:acetonitrile buffered solution (0.02 M HEPES buffer, pH 7, T = 25 °C). In a typical experiment, incremental amounts of a solution of the chosen anion were added to a 50 μM solution of the [Cu₂L](CF₃SO₃)₄ complex (10 cm quartz cuvette, 25 ml, path length = 10 cm), and the corresponding UV-Vis spectra were recorded using a Varian Cary 50 SCAN spectrophotometer. Titration data were fitted with the Hyperquad package [4] to estimate equilibrium constants.

The same procedure was followed for the UV-Vis titration of the fluorescent indicator 6-carboxytetramethylrhodamine (6-TAMRA, 0.25 μM) with [Cu₂L](CF₃SO₃)₄ in 1:4 (*v/v*) H₂O:CH₃CN buffered solution (0.02 M HEPES buffer) in a 1 cm quartz cuvette.

76



77

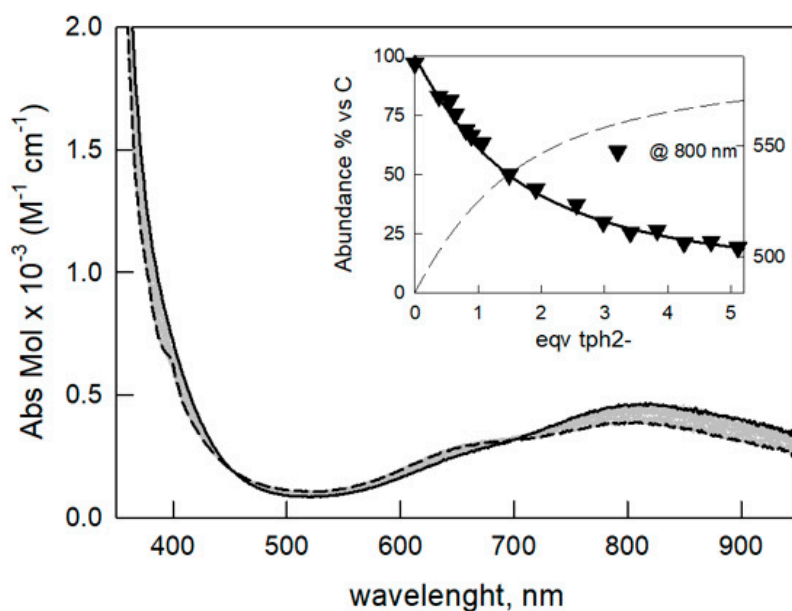
78

79

80

81

Figure S2. UV-Vis spectra taken upon titration of $[\text{Cu}_2\text{L}](\text{CF}_3\text{SO}_3)_4$ ($50\ \mu\text{M}$) with sdbz^{2-} (as the TBA salt) in $\text{H}_2\text{O}:\text{CH}_3\text{CN}$ 1:4 at pH 7 (0.02 M HEPES buffer; path length = 10 cm). The inset shows the titration profiles at 650 and 800 nm, with the superimposed distribution diagram of the dicopper complex containing species: dotted line, $[\text{Cu}_2\text{L}(\text{sdbz})]^{2+}$; solid line, $[\text{Cu}_2\text{L}]^{4+}$; $\text{Log}K_{11} = 5.08(1)$.



82

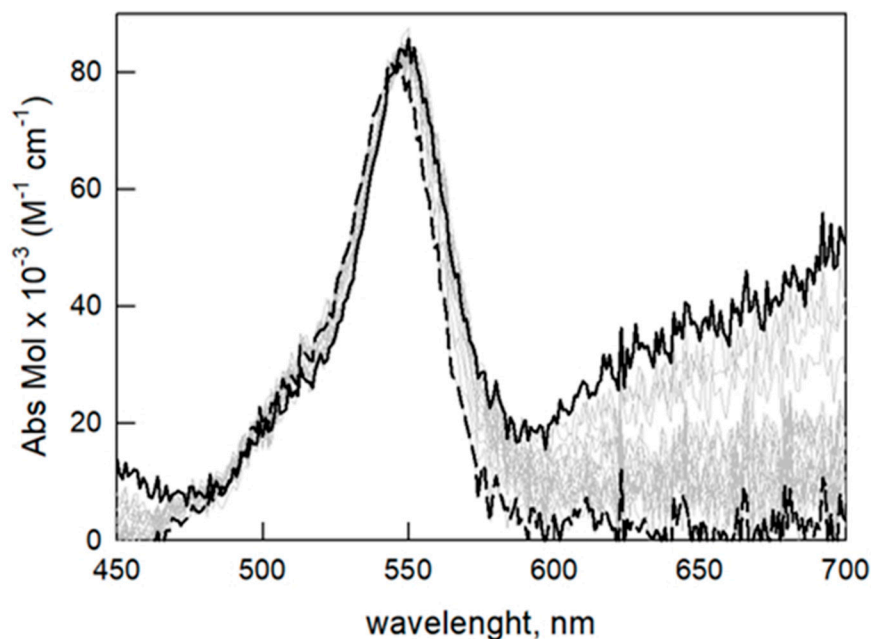
83

84

85

86

Figure S3. UV-Vis spectra taken upon titration of $[\text{Cu}_2\text{L}](\text{CF}_3\text{SO}_3)_4$ ($50\ \mu\text{M}$) with tph^{2-} (as the TBA salt) in $\text{H}_2\text{O}:\text{CH}_3\text{CN}$ 1:4 at pH 7 (0.02 M HEPES buffer; path length = 10 cm). The inset shows the titration profiles at 800 nm, with the superimposed distribution diagram of the dicopper complex containing species: dotted line, $[\text{Cu}_2\text{L}(\text{tph})]^{2+}$; solid line, $[\text{Cu}_2\text{L}]^{4+}$; $\text{Log}K_{11} = 4.43(4)$.



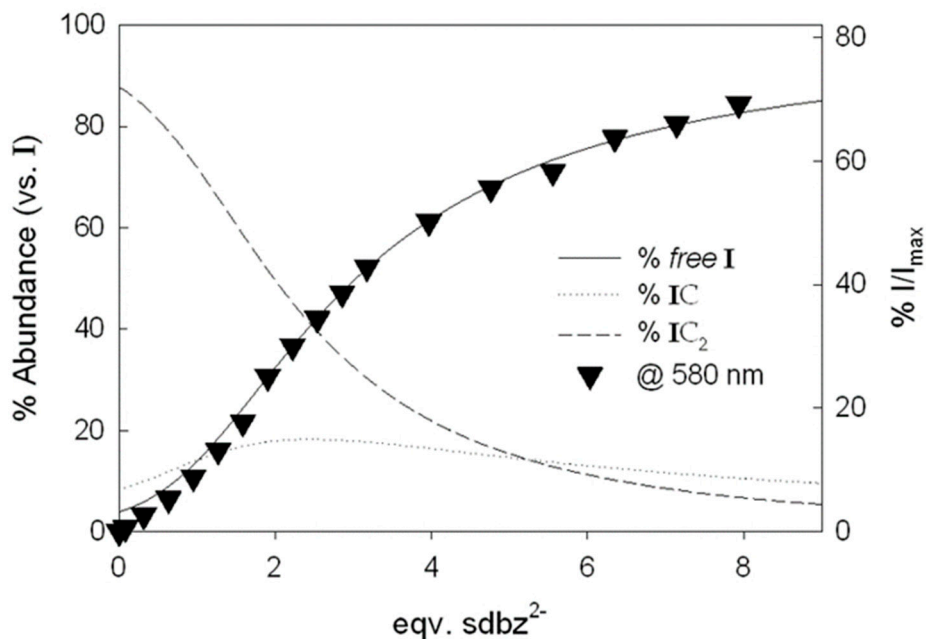
87

88 **Figure S4.** Family of UV-Vis spectra recorded during the titration of 6-TAMRA (0.25 μM , path length
89 = 1 cm) with $[\text{Cu}_2\text{L}](\text{CF}_3\text{SO}_3)_4$ in $\text{H}_2\text{O}:\text{CH}_3\text{CN}$ 1:4 at pH 7 (0.02 M HEPES buffer).

90 2.3 Emission Studies

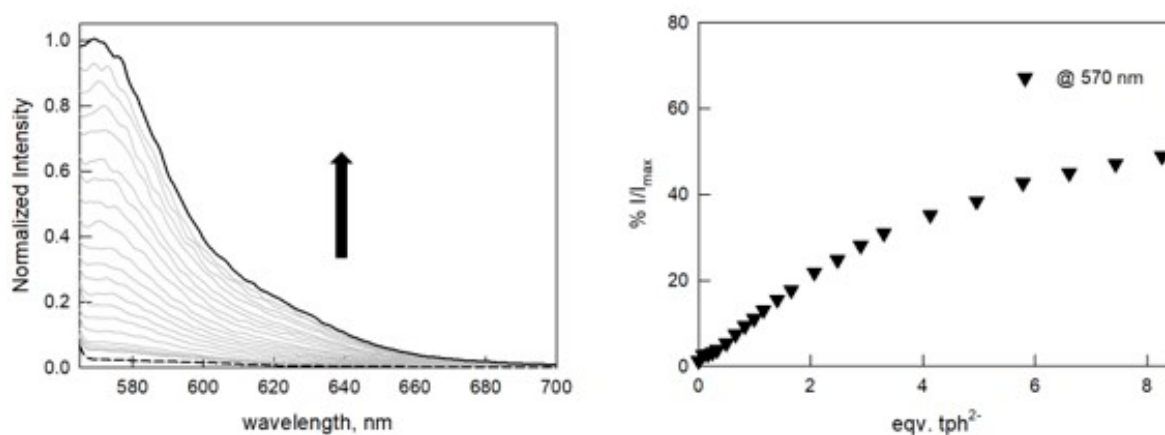
91 Emission spectra were recorded on a PerkinElmer LS 50B instrument. Fluorimetric titration of
92 6-TAMRA (I, $\lambda_{\text{exc}} = 548$ nm) with $[\text{Cu}_2\text{L}](\text{CF}_3\text{SO}_3)_4$ (C) were performed in 1:4 $\text{H}_2\text{O}:\text{CH}_3\text{CN}$ buffered
93 solution (0.02 M HEPES buffer, pH 7) in a 1 cm quartz cuvette: an incremental amount of the complex
94 solution was added to a 0.25 μM solution of indicator (stored in the dark) and the corresponding
95 emission spectra were recorded. The fluorescent intensity was normalized at 570 nm.

96 For competition assays with dicarboxylate species, a chemosensing ensemble solution was
97 prepared by mixing C (50 μM) and I (0.25 μM) in 1:4 $\text{H}_2\text{O}:\text{CH}_3\text{CN}$ buffered solution (0.02 M HEPES
98 buffer, pH 7). In these conditions, the emission of 6-TAMRA was totally quenched (fluorescence
99 intensity normalized at 570 nm). An increasing amount of a solution of the chosen anion was added
100 to the chemosensing ensemble solution and the corresponding emission spectra were recorded.
101 Titration data were fitted with the Hyperquad package [4] to estimate equilibrium constants.



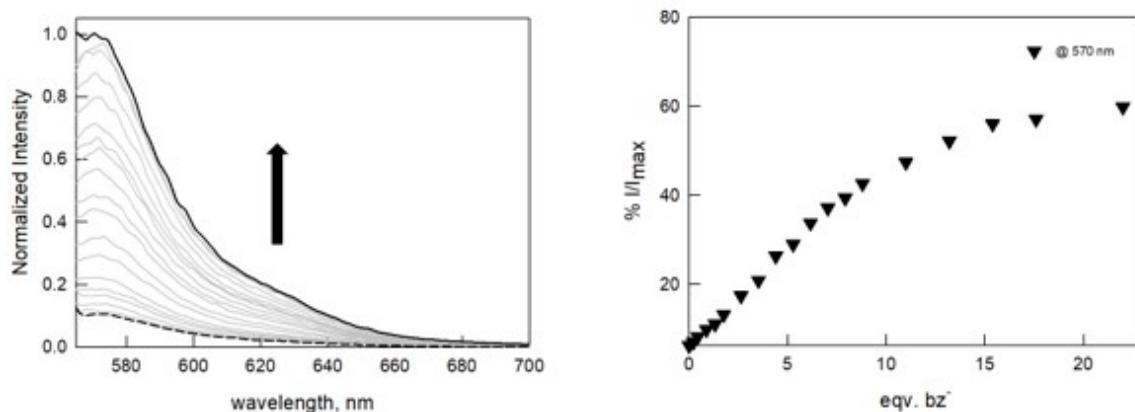
102
103
104
105
106
107
108

Figure S5. Fluorimetric titration of the chemosensing ensemble solution ($0.25 \mu\text{M I}$; $50 \mu\text{M C}$, $\lambda_{\text{exc}} = 548 \text{ nm}$) with sdbz^{2-} (as the TBA salt) in $\text{H}_2\text{O}:\text{CH}_3\text{CN}$ 1:4 at pH 7 (0.02 M HEPES buffer). The titration profile (left), as % I/I_{max} (I_{max} = emission intensity of I in the absence of C) vs. eqv. of the dicarboxylate anion, with the superimposed distribution diagram of the indicator containing species (I = 6-TAMRA; C = $[\text{Cu}_2\text{L}]^{4+}$; IC and $\text{IC}_2 = 1:1$ and $1:2$ I:C adducts, respectively). The distribution diagram was obtained using the equilibrium constants reported in Table 1 and in the text.



109
110
111
112
113

Figure S6. Normalized emission spectra (right) taken upon titration of the chemosensing ensemble solution ($0.25 \mu\text{M I}$; $50 \mu\text{M C}$, $\lambda_{\text{exc}} = 548 \text{ nm}$) with tph^{2-} (as the TBA salt) in $\text{H}_2\text{O}:\text{CH}_3\text{CN}$ 1:4 at pH 7 (0.02 M HEPES buffer). The titration profile (left), as % I/I_{max} (I_{max} = emission intensity of I in the absence of C) vs. eqv. of the dicarboxylate anion.

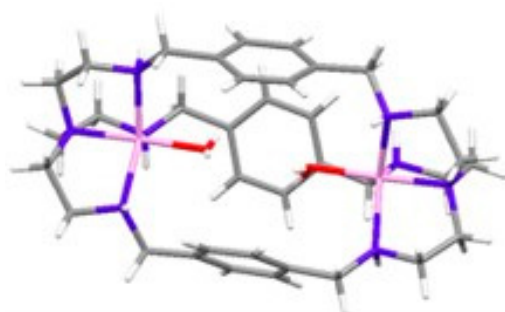


114

115 **Figure S7.** Normalized emission spectra (right) taken upon titration of the chemosensing ensemble
 116 solution (0.25 μM I; 50 μM C, $\lambda_{\text{exc}} = 548 \text{ nm}$) with bz⁻ (as the TBA salt) in H₂O:CH₃CN 1:4 at pH 7 (0.02
 117 M HEPES buffer). The titration profile (left), as % I/I_{max} (I_{max}= emission intensity of I in the absence of
 118 C) vs. eqv. of the dicarboxylate anion.

119 3. Computational Studies

120 All the computational studies were carried out using the GAUSSIAN09 program package [5].
 121 The structures were optimized in the gas phase at the B3LYP/6-31 G level of theory.
 122



X-ray structure

Cu-N distances: 2.00 Å (tertiary amine),
 2.20, 2.10 Å (secondary amines).
 Cu-Cu distance: 7.01 Å
 H₂O-OH₂ distance: 3.03 Å

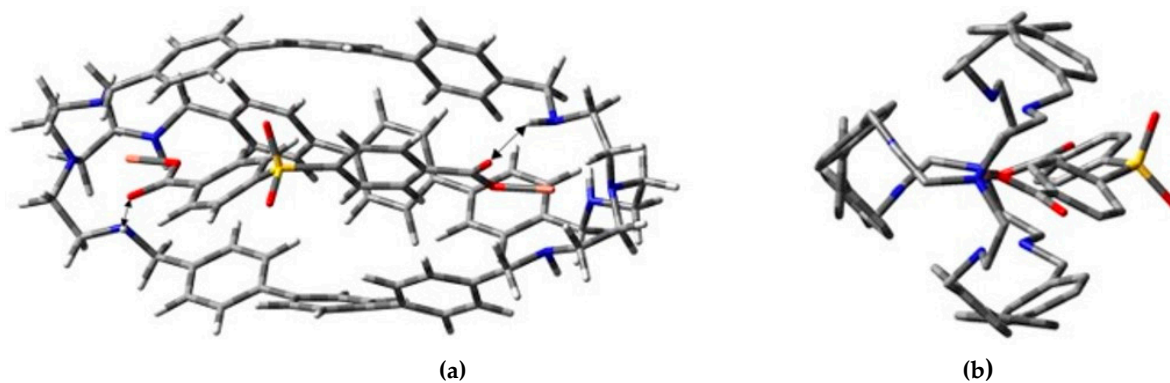


Calculated structure

Cu-N distances: 2.00 Å (tertiary amine),
 2.19, 2.12 Å (secondary amines).
 Cu-Cu distance: 7.25 Å
 H₂O-OH₂ distance: 3.33 Å

123

124 **Figure S8.** Comparison between crystal and calculated structures for the complex [Cu₂L'(H₂O)₂]⁴⁺ (L'
 125 = bisten azacryptand with p-xylyl spacers).

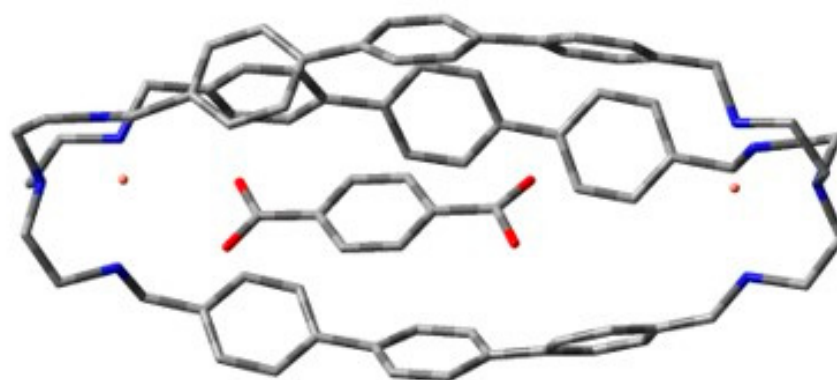


126

127

Figure S9. Lateral (a) and front (b) view of the calculated structure of the complex $[\text{Cu}_2\text{L}(\text{sdbz})]^{2+}$.

128



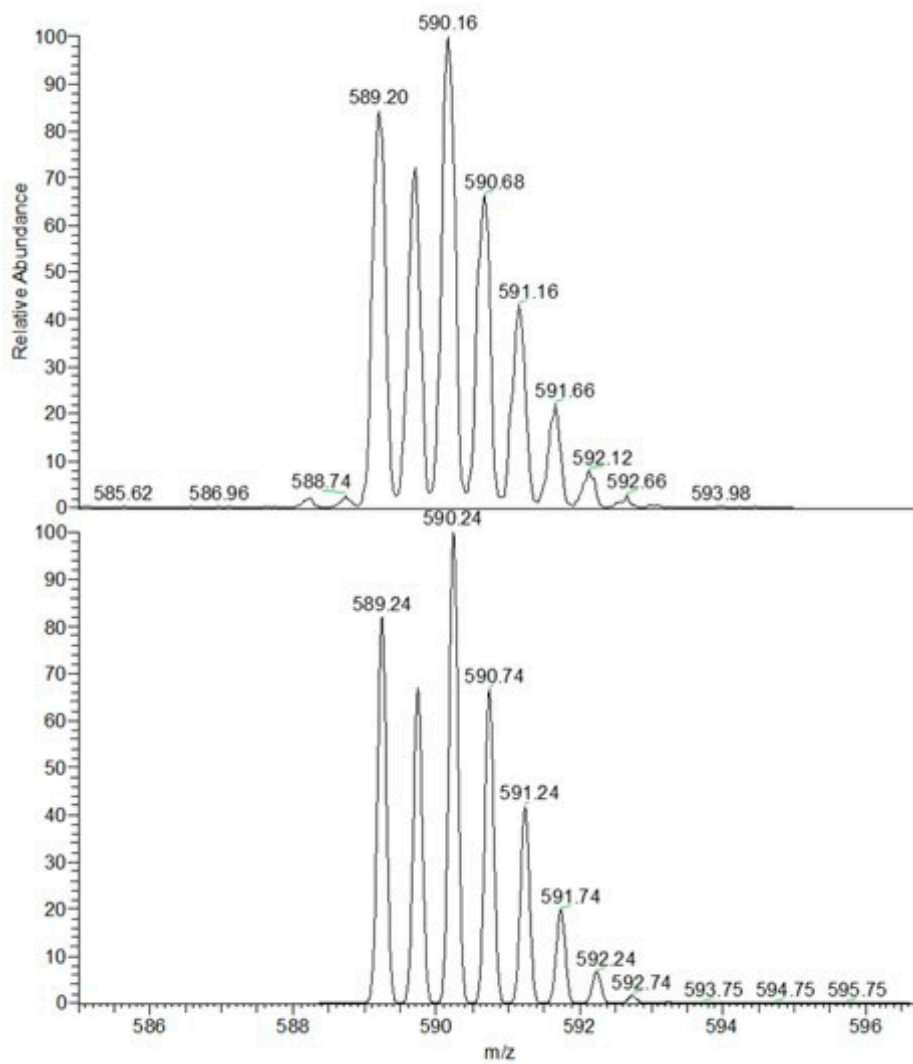
129

130

131

Figure S10. Lateral view of the calculated structure of the complex $[\text{Cu}_2\text{L}(\text{tph})]^{2+}$.

132

133 4. Characterization of $[\text{Cu}_2\text{L}]^{4+}$ by ESI-MS

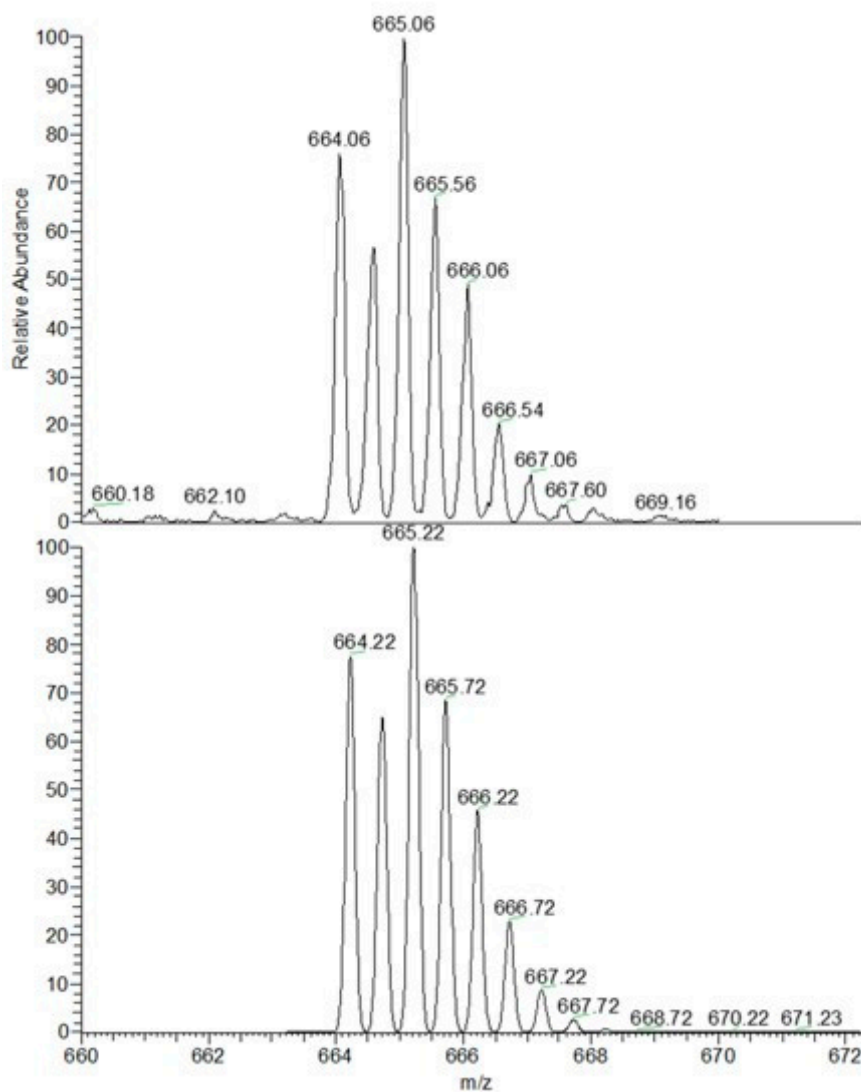
134

135

136

137

Figure S11. Top: zoom scan of the peak at 590 m/z , obtained from the experimental ESI-MS spectrum of a solution of $[\text{Cu}_2\text{L}(\text{CF}_3\text{SO}_3)_4]$ in $\text{CH}_3\text{CN}:\text{H}_2\text{O}$ 4:1. **Bottom:** simulated peak, calculated for the species $[\text{Cu}_2\text{C}_{72}\text{H}_{76}\text{N}_8]^{2+}$ (i.e., $[\text{Cu}^{\text{II}}_2(\text{L}-2\text{H}^+)]^{2+}$).



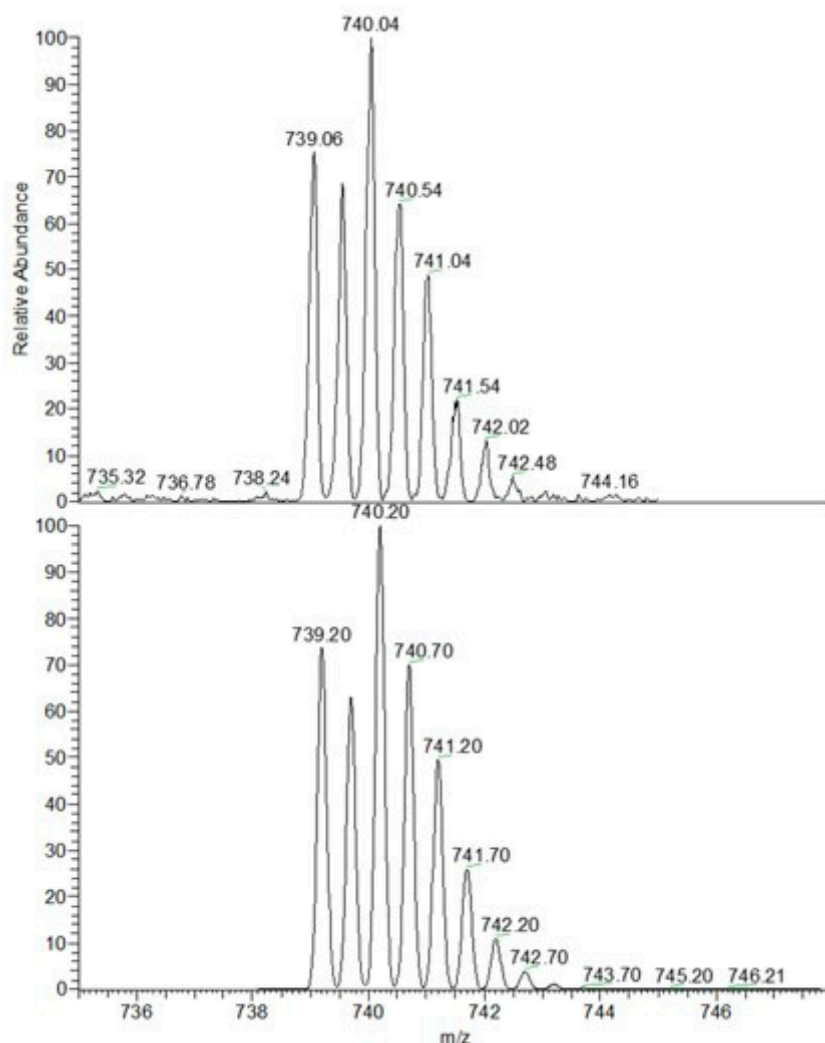
138

139

140

141

Figure S12. Top: zoom scan of the peak at 665 m/z , obtained from the experimental ESI-MS spectrum of a solution of $[\text{Cu}_2\text{L}(\text{CF}_3\text{SO}_3)_4]$ in $\text{CH}_3\text{CN}:\text{H}_2\text{O}$ 4:1. **Bottom:** simulated peak, calculated for the species $[\text{Cu}_2\text{C}_{73}\text{H}_{77}\text{N}_8\text{O}_3\text{F}_3\text{S}]^{2+}$ (i.e., $[\text{Cu}^{\text{II}}_2(\text{L}-\text{H}+\text{CF}_3\text{SO}_3)]^{2+}$).



142

143

144

145

Figure S13. Top: zoom scan of the peak at 740 m/z , obtained from the experimental ESI-MS spectrum of a solution of $[\text{Cu}_2\text{L}(\text{CF}_3\text{SO}_3)_4]$ in $\text{CH}_3\text{CN}:\text{H}_2\text{O}$ 4:1. **Bottom:** simulated peak, calculated for the species $[\text{Cu}_2\text{C}_{74}\text{H}_{78}\text{N}_8\text{O}_6\text{F}_6\text{S}_2]^{2+}$ (i.e., $[\text{Cu}^{II}_2\text{L}(\text{CF}_3\text{SO}_3)_2]^{2+}$).

146

147

148

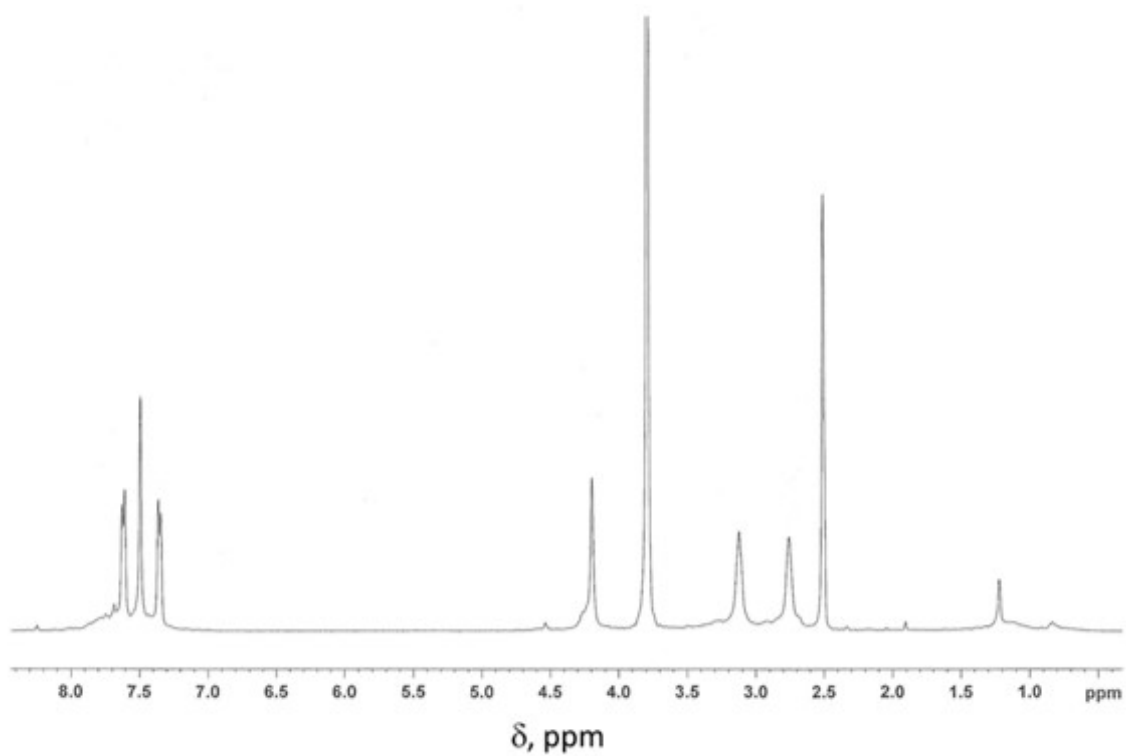
149

150

151

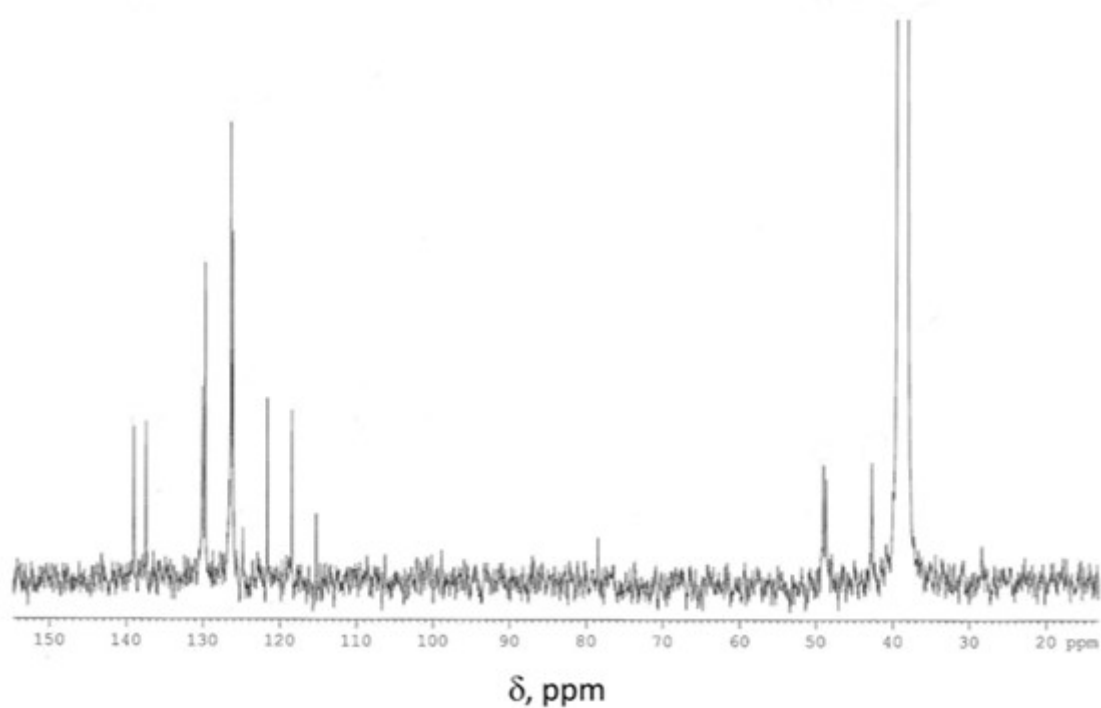
In the case of dicopper complex, the ESI-MS studies revealed the presence of three double-charged species, in which both copper centers are in the +2 oxidation state, but in the first case (peak at 590 m/z) the ligand is doubly deprotonated ($[\text{Cu}^{II}_2(\text{L}-2\text{H}^+)]^{2+}$), while in the second case (665 m/z) is once deprotonated ($[\text{Cu}^{II}_2(\text{L}-\text{H}^+\text{CF}_3\text{SO}_3)]^{2+}$). Notably, this process (i.e., ligand deprotonation) is common in the ESI-MS spectra of copper complexes with polyamine ligands, especially when using MeOH as solvent [6].

152 5. NMR Characterization of L



153

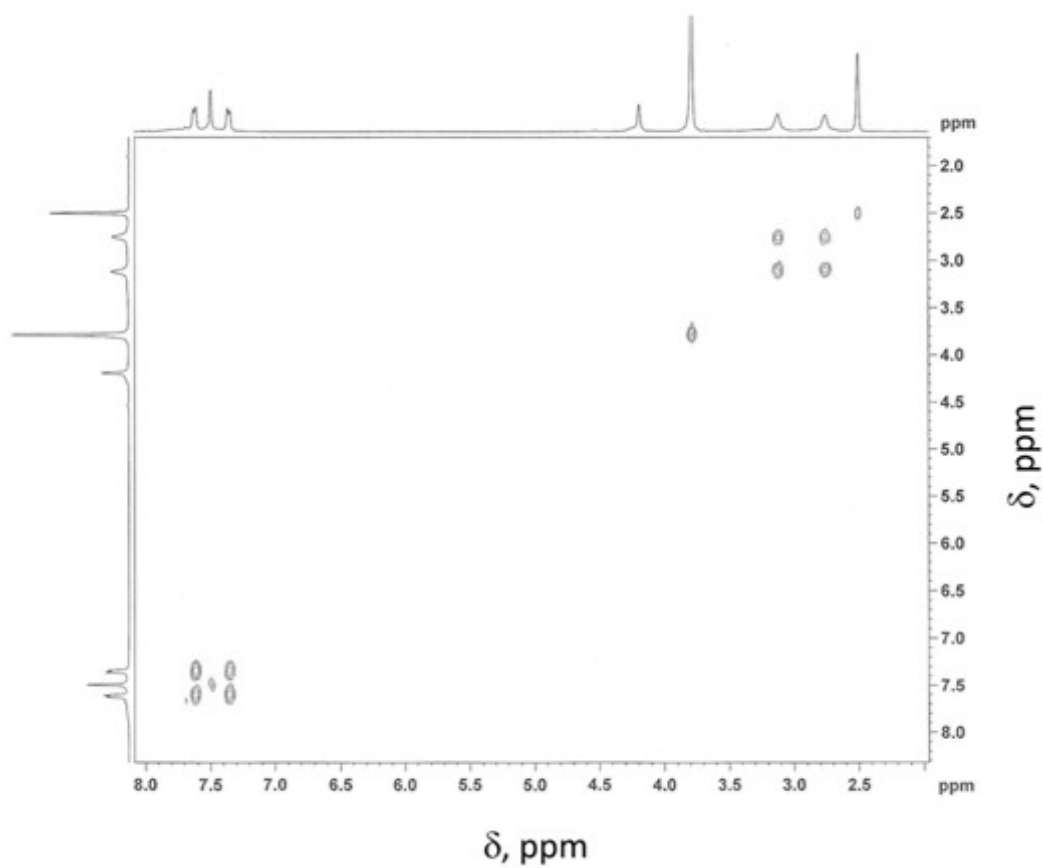
154

Figure S14. ¹H-NMR spectra of L in d₆-DMSO + 1M CF₃SO₃H in D₂O.

155

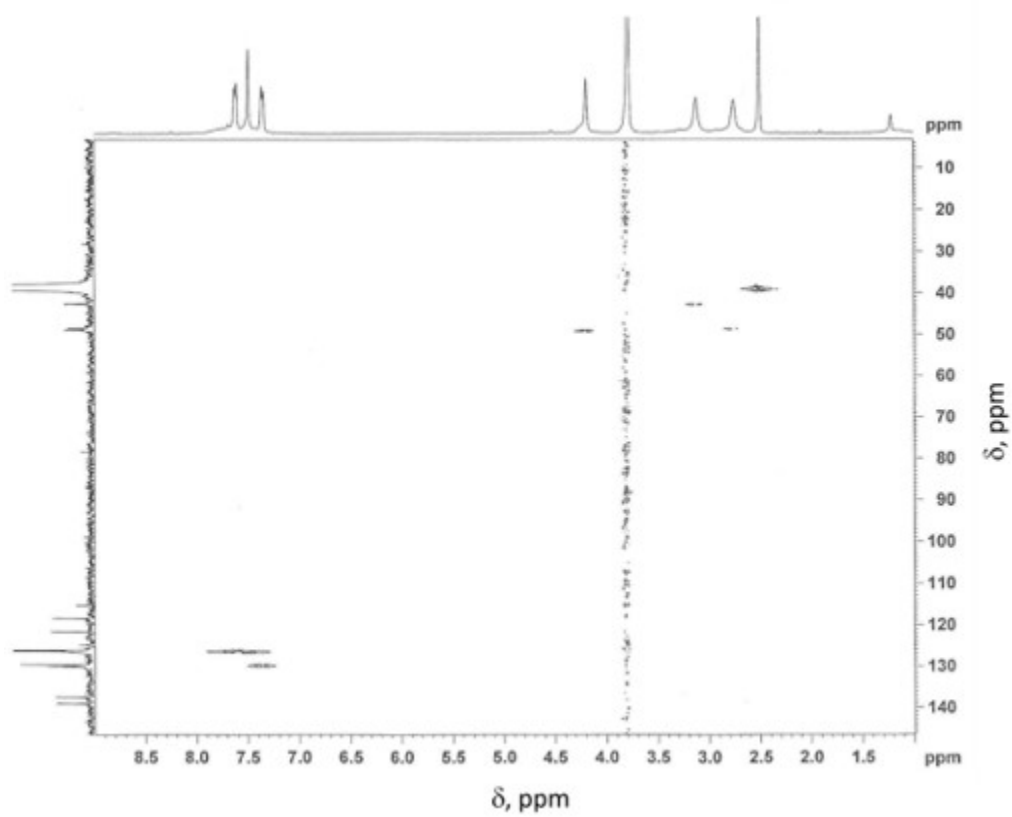
156

Figure S15. ¹³C-NMR spectra of L in d₆-DMSO + 1M CF₃SO₃H in D₂O.



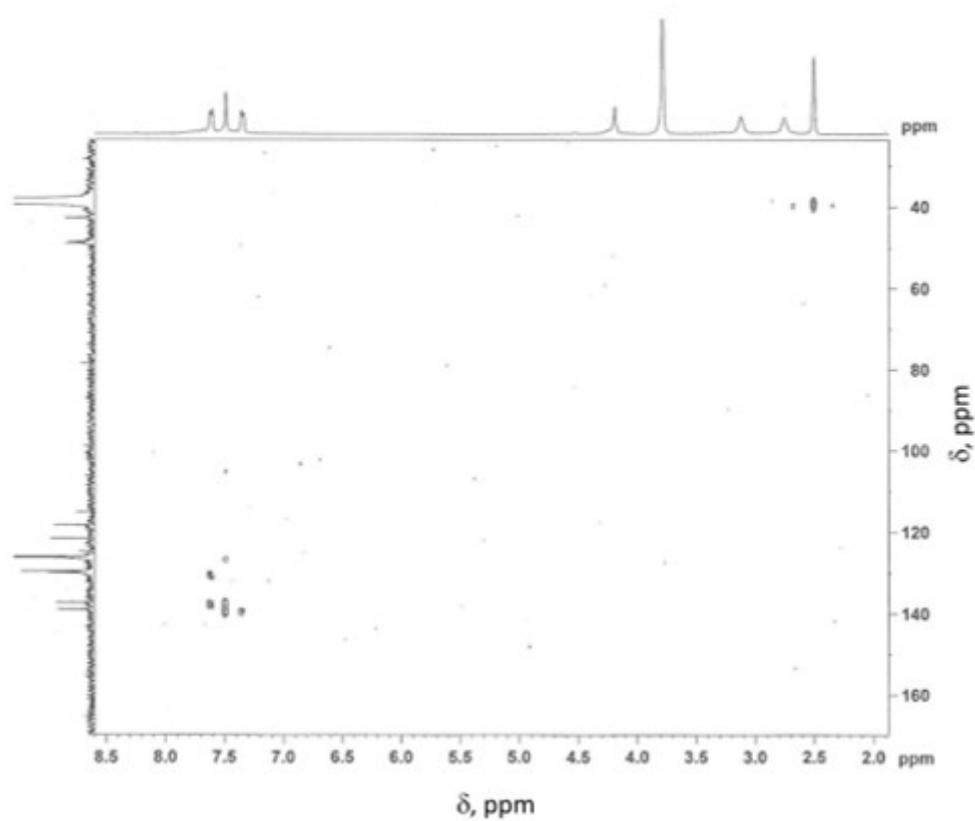
157
158

Figure S16. ^1H - ^1H COSY spectrum of L in d_6 -DMSO + 1M $\text{CF}_3\text{SO}_3\text{H}$ in D_2O .



159
160

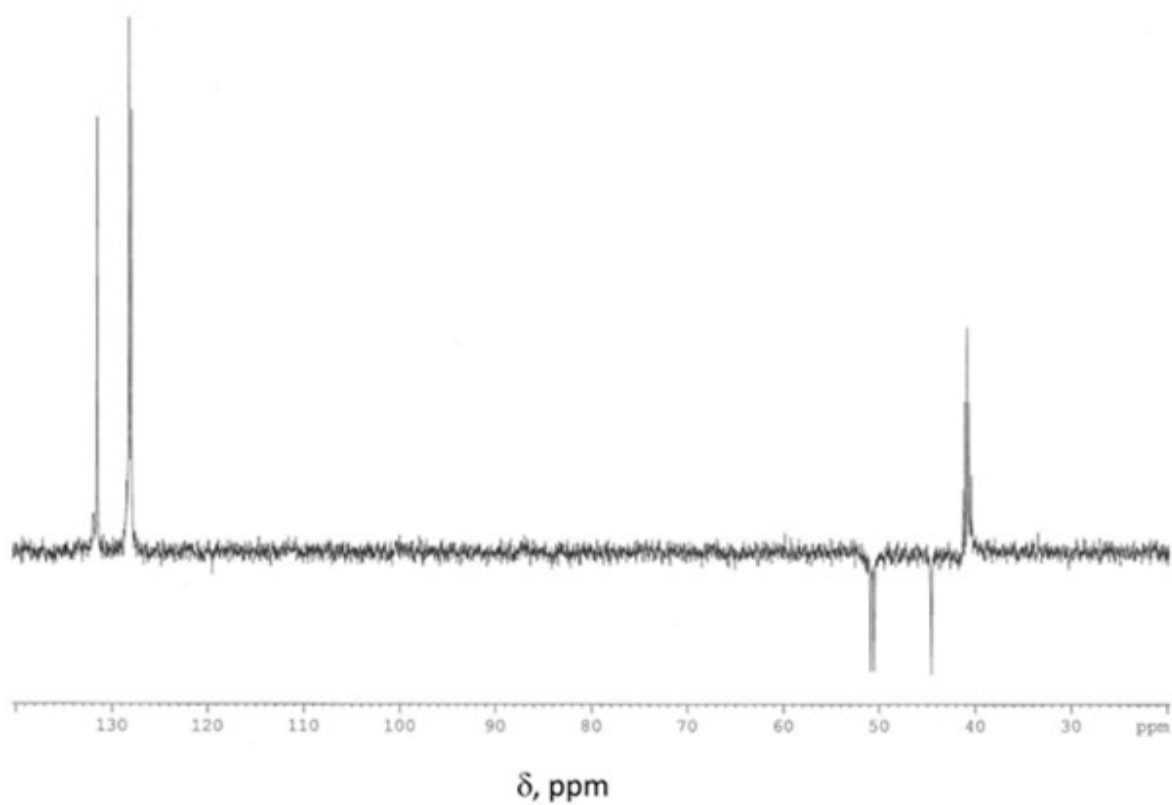
Figure S17. ^1H - ^{13}C -HSQC spectrum of L in d_6 -DMSO + 1M $\text{CF}_3\text{SO}_3\text{H}$ in D_2O .



161

162

Figure S18. ^1H - ^{13}C -HMBC spectrum of L in d_6 -DMSO + 1M $\text{CF}_3\text{SO}_3\text{H}$ in D_2O .



163

164

Figure S19. DEPT135 of L in d_6 -DMSO + 1M $\text{CF}_3\text{SO}_3\text{H}$ in D_2O .

165 **References**

- 166 1. Bounos, G.; Ghosh, S.; Lee, A.K.; Plunkett, K.N.; DuBay, K.H.; Bolinger, J.C.; Zhang, R.;
167 Friesner, R.A.; Nuckolls, C.; Reichman, D.R.; et al. Controlling Chain Conformation in Conjugated
168 Polymers Using Defect Inclusion Strategies. *J. Am. Chem. Soc.* **2011**, *133*, 10155–10160;
169 DOI:10.1021/ja2006687.
- 170 2. Borch, R.F.; Bernstein, M.D.; Durst, H.D. Cyanohydridoborate anion as a selective reducing
171 agent. *J. Am. Chem. Soc.* **1971**, *93*, 2897–2904; DOI:10.1021/ja00741a013.
- 172 3. Gran, G. Determination of the equivalence point in potentiometric titrations. Part II *Analyst* **1952**,
173 *77*, 661–671.
- 174
- 175 4. Gans, P.; Sabatini, A.; Vacca, A. Investigation of equilibria in solution. Determination of
176 equilibrium constants with the HYPERQUAD suite of programs. *Talanta* **1996**, *43*, 1739–1753;
177 DOI:10.1016/0039-9140(96)01958-3.
- 178 5. Frisch, M.J.; Trucks, J.W.; Schlegel, H.B.; Scuseria, G.E.; Robb, M.A.; Cheeseman, J.R.;
179 Scalmani, G.; Barone, V.; Mennucci, B.; Petersson, G.A.; et al. *Gaussian 09*; Gaussian, Inc.:
180 Wallingford CT, USA, 2009.
- 181 6. Gianelli, L.; Amendola, V.; Fabbrizzi, L.; Pallavicini, P.; Mellerio, G.G. Investigation of
182 reduction of Cu(II) complexes in positive-ion mode electrospray mass spectrometry. *Rapid*
183 *Communications in Mass Spectrometry* **2001**, *15*, 2347–2353; DOI:10.1002/rcm.510.